

# Determination of the Mechanical Properties in the Avian Middle Ear by Inverse Analysis

P. Muyshondt<sup>\*1</sup>, D. De Greef<sup>1</sup>, J. Soons<sup>1</sup>, J. Peacock<sup>1</sup>, and J.J.J. Dirckx<sup>1</sup>

<sup>1</sup>University of Antwerp, Laboratory of Biomedical Physics

<sup>\*</sup>Groenenborgerlaan 171, B-2020 Antwerp, Belgium, pieter.muyshondt@student.uantwerpen.be

**Abstract:** This paper presents the study of the avian middle ear as a biomechanical system, which is typically made up of a single hearing ossicle, the columella. So far, only few is known about the functioning of the avian middle ear. To gain new information about the mechanical properties of this system, a finite element model was created using a viscoelastic characterization, for which the geometry was extracted from  $\mu$ CT scans recorded from the middle ear of a mallard duck. Some of the unknown model parameters were determined by performing an inverse analysis, in which the model output is compared with the outcome of optical interferometric experiments, like stroboscopic digital holography and laser Doppler vibrometry. As a result of this procedure, several parameter values of different middle ear structures could be found.

**Keywords:** middle ear mechanics, finite element modeling, optical interferometry, inverse analysis.

## 1. Introduction

The avian middle ear is a peculiar biomechanical system that serves as an impedance match between incoming sound waves in air and acoustic waves in the inner ear fluid. In contrast to the mammalian middle ear, which contains three ossicles and a number of muscles and ligaments, the avian middle ear only contains a single ossicle, called the columella, one muscle and one prominent ligament (see Fig. 1). Despite this far simpler design, birds are able to perceive sound signals in a frequency range that is almost as broad as mammals [1, 2]. Despite these interesting properties, the avian middle ear has not been given the same research attention as the mammalian middle ear.

This paper presents the current state of our research of avian middle ear mechanics through stroboscopic digital holography, laser Doppler vibrometry (LDV) and finite element modeling. The model's geometry is deduced from  $\mu$ CT measurements and its parameters are optimized

using the experimental results. The work will provide novel insights in the functioning of this mechanically simpler variant to mammal middle ears, and therefore have important consequences in the development of middle ear ossicular replacement prostheses. Because some of the current middle ear prostheses designs (such as a TORP - Total Ossicle Replacement Prosthesis) qualitatively resemble the avian middle ear [3], studying this system will assist in determining the optimal shape, parameters, material choice and placement of these prostheses.

## 2. Methods

### 2.1 Numerical Model

To start with, the model's geometry was obtained from  $\mu$ CT measurements at the UGCT, UGhent [4], performed on a segment of the left skull half of a dead mallard duck, with a resolution of 7.5  $\mu$ m. In order to enhance the X-ray contrast of different types of soft tissue, the sample was stained in a daily refreshed 2.5% PTA (Phosphotungstic acid) solution in deionized water for 48 hours before the scan. From these data, different middle ear structures were segmented using Amira (Visage Imaging) to create a surface model of the middle ear which is needed to create a realistic numerical model.

Within the surface model, as depicted on Fig. 2, five different structures could be distinguished: the tympanic membrane, Platner's ligament, the cartilaginous extracolumella and the bony columella with the footplate bounded by an annular ligament. Other ligaments mentioned in literature were not observed and therefore not considered in the geometry. The final geometrical surface model, consisting of 15000 triangle-shaped faces after decimation and smoothing of the surface, was exported as an STL-file that could be imported in finite element software (COMSOL Multiphysics 4.3b, The Structural Mechanics Module) in order to create a mechanical model.

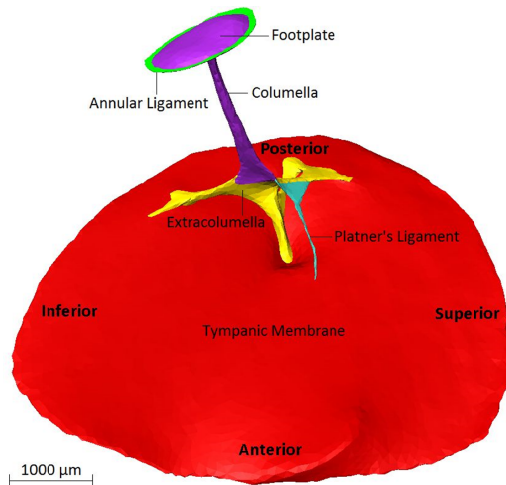


**Figure 1.** Geometrical surface model of the left middle ear of a mallard duck, reconstructed from  $\mu$ CT measurements. The different components and anatomical orientations are indicated [5].

Finite element studies of the human middle ear have indicated that a viscoelastic characterization of the soft tissue structures is necessary to predict the observed behavior [6]. Therefore, we chose to introduce a complex elastic modulus with an isotropic loss factor. Since there are no literature values available for the elastic parameters of the avian middle ear, human and other viscoelastic material parameters were used as initial values instead. As explained in the next section, some of these parameters will be optimized using the experimental data. In table 1 starting values for different parameters of all components are listed. Initially, all parameters were chosen isotropic.

**Table 1:** Starting material parameters used in the finite element model. All mass densities  $\rho$  and Poisson's ratios  $\nu$  are taken from [7]. Values for the Young's modulus  $E$  indicated with <sup>a</sup> are taken from [7]; <sup>b</sup> taken from [8]; <sup>c</sup> taken from [9] and <sup>d</sup> taken from [10]. All loss factors  $\eta_s$  come from [6], except for <sup>d</sup> coming from [10].

Component	$\rho$ [kg/m <sup>3</sup> ]	$E$ [MPa]	$\eta_s$	$\nu$
TM	1.2E3	20 <sup>a</sup>	0.078	0.3
Columella	2.2E3	1410 <sup>a</sup>	0 <sup>d</sup>	0.3
Extracol.	1.2E3	39.2 <sup>b</sup>	0.078	0.3
Platner's lig.	1.2E3	21 <sup>c</sup>	0.078	0.3
Annular lig.	1.2E3	0.0412 <sup>a</sup>	0.078	0.3

The finite element model was built up by two types of mesh elements: 2D triangle-shaped shell elements for the tympanic membrane, which are appropriate for thin structures, and 3D tetrahedral solid elements for the remaining middle ear components, as depicted in Fig. 2. Because shell elements are only two-dimensional, one needs a procedure to account for the finite and variable thickness of the tympanic membrane. This was realized by defining a function on the eardrum elements that interpolates the thickness distribution obtained from the original image segmentation data, as shown on Fig. 3. Despite the two-dimensional mathematical framework of shell elements, they still account for typical three-dimensional properties like bending stiffness and inertia.

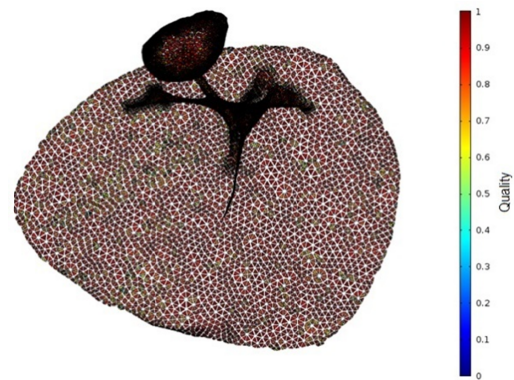


**Figure 2.** Applied mesh in the finite element model. Shell elements are used for the tympanic membrane and solid elements for the remaining components. The colors represent element quality.

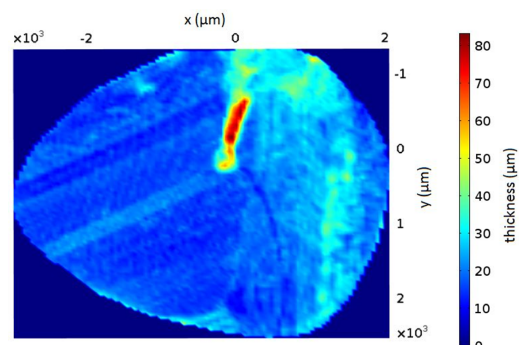


**Figure 3.** Interpolation function containing the thickness distribution of the tympanic membrane, which is defined on the according shell elements in Fig. 2 [5].

To model the incident acoustic waves at the tympanic membrane, a uniform harmonic load of 1 Pa was applied at the outer (i.e. lateral) surface of the eardrum. To account for the reflection of sound energy at the tympanic membrane, an empirically measured and frequency dependent power utilization ratio [11] was defined at the eardrum, so that only a part of the acoustic waves is actually transmitted to the middle ear. The presence of the cochlea in the inner ear behind the columella footplate was simulated by a viscoelastic spring foundation that was introduced at the footplate to account for the impedance caused by the cochlear fluid [12].

The tympanic membrane was fully constrained at the edge, as well as the annular ligament and the end of Platner's ligament. To determine the linear response from the middle ear to harmonic loads, the computations were performed in the frequency domain. From these calculations the resulting displacement magnitude and phase over the entire eardrum were deduced.

To validate the finite element model, the vibrating motion of the mallard middle ear was measured under acoustic stimulation, using both stroboscopic digital holography and laser Doppler vibrometry as experimental tools. These optical techniques allow us to measure the full-field displacement and the single-point velocity amplitude of an object's surface respectively. More detail on these techniques can be found in previous work [5, 13].

## 2.2 Inverse Analysis

As mentioned before, there are no avian middle ear properties available in literature. Therefore, the mechanical parameters of the middle ear components were validated by performing an inverse analysis routine in which the finite element model is compared with the experimental results. In this procedure the aim is to optimize the model in a certain way so that it approximates the experiment as well as possible. Therefore, an intelligently defined objective function is to be minimized. The objective function that was minimized using the holography measurements is defined as

$$f^2(p) = \sum_i \left[ \left( M_{\text{mod}}(r_i, p) - M_{\text{exp}}(r_i) \right)^2 + \left( \phi_{\text{mod}}(r_i, p) - \phi_{\text{exp}}(r_i) \right)^2 \right]. \quad (1)$$

In this equation the summation index  $i$  runs over the number of evaluated points on the eardrum surface. The  $r_i$  represent the spatial coordinates on the eardrum and  $p$  is the set of model parameters to be optimized.  $M$  represents the magnitude normalized to 1 and  $\phi$  the vibration phase in cycles (between 0 and 1). The subscripts 'mod' and 'exp' denote model and experimental results, respectively. Magnitude maps were normalized to their respective maximal magnitude to prevent erroneously large values for the objective function.

Using the LDV measurements as input for the inverse analysis instead, the objective function can be defined as

$$f^2(p) = \sum_i \left( V_{\text{mod}}(\omega_i, p) - V_{\text{exp}}(\omega_i) \right)^2. \quad (2)$$

In this equation  $V$  represents the velocity magnitude at the center of the columella. The summation no longer runs over the space coordinates  $r_i$ , but over the applied stimulus frequencies  $\omega_i$ .

The technique that is employed to perform the optimization is called surrogate modeling, for which we used the MATLAB Surrogate Modeling (SUMO) Toolbox, developed by INTEC, UGhent [14]. To operate COMSOL and SUMO simultaneously, we made use of the COMSOL LiveLink for MATLAB. The surrogate modeling technique creates a model of a certain system for which we only know the input and output. The software achieves this by first choosing a set of initial input samples, based on a so called Latin Hypercube Design, and calculating the according output. It then builds a model through the resulting evaluated samples by use of the Kriging Modeling technique. From the obtained model the software chooses new samples to evaluate in order to improve the current surrogate model. The way these new samples are chosen is done by the Local Linear Addaptive Sampling Algorithm (LOLA), which identifies nonlinear regions in the current surrogate model to evaluate them more densely. A second routine, called the Dividing Rectangles Algorithm, determines the current minima of the model and evaluates them. This procedure is repeated until a certain tolerance is reached or when a maximum number of samples have been evaluated. The complete workflow is summarized on Fig. 4.

The parameters that are to be optimized still have to be chosen. This is done by the

application of manual sensitivity tests, in which the change in model output is evaluated after changing the input parameter values. The parameters that influence the output most, will eventually be optimized. For the holography results, the total objective function of Eq. (1), and therefore also the resulting optimization, will be computed for the different applied sound frequencies separately, since viscoelastic parameters are known to be frequency dependent.

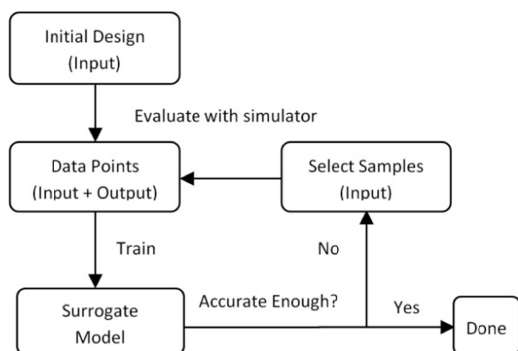


**Figure 4.** The workflow of a surrogate modeling routine for a certain system with input and output. Taken from the SUMO Toolbox Tutorial, Ivo Couckuyt, INTEC UGhent [14].

### 3. Results

#### 3.1 Experimental Results

In order to interpret the results from digital holography, a temporal FFT-analysis is applied to the time-dependent displacement maps that are obtained from the experiments. From this analysis, vibration magnitude and phase relative to the sound signal at the TM are calculated for each object point. The results are presented in Fig. 5 as magnitude and phase maps for different stimulus frequencies.

Fig. 6 shows the result from LDV measurements on the center of the columella footplate. The figure presents footplate velocity magnitude as a function of input frequency. The sound pressure was kept at 90 dB SPL for all frequencies. The two distinct resonance peaks of roughly the same height are remarkable, as mammalian middle ear transfer functions typically feature only one high resonance peak and multiple subsequent smaller peaks at higher frequencies.

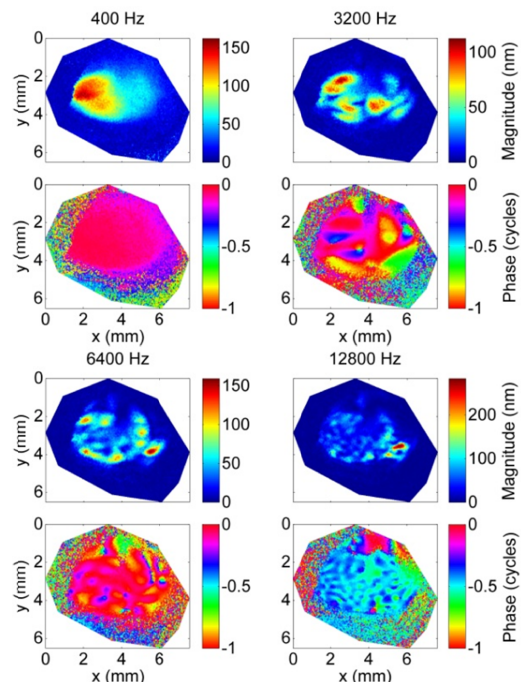


**Figure 5.** Displacement magnitude and phase maps of the duck eardrum, extracted from digital holography data at different frequencies.

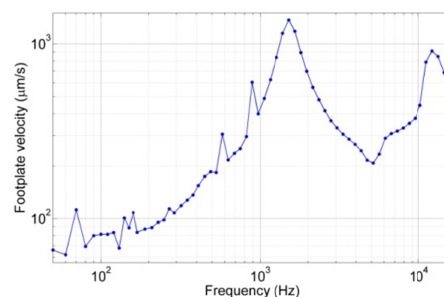


**Figure 6.** Velocity of the center point of the columella footplate, derived from LDV measurements. The sound pressure for all frequencies was 90 dB SPL [5].

#### 3.2 Model Results

This section contains results of the inverse analysis on the finite element model, based on the holography and LDV measurements. First of all, a surrogate modeling routine was carried out on the objective function between model and experiment, as defined by Eq. (1). The input parameters incorporated in this procedure were chosen to be the Young's moduli of the eardrum and the extracolumella, as a result of the sensitivity tests. The calculations were executed



for the different applied sound frequencies separately, and results are shown for the example frequency of 1600 Hz in Fig. 7.

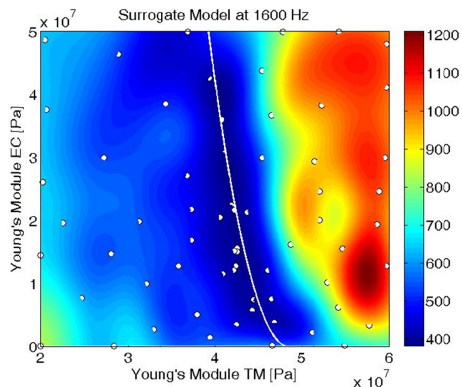


**Figure 7.** Inverse analysis on the Young's moduli of the tympanic membrane (TM) and the extracolumella (EC) at the sound frequency of 1600 Hz. The result is obtained by a surrogate modeling routine built with 64 samples. Colors on the plot represent the objective function between model and experiment as defined by Eq. (1) [5].

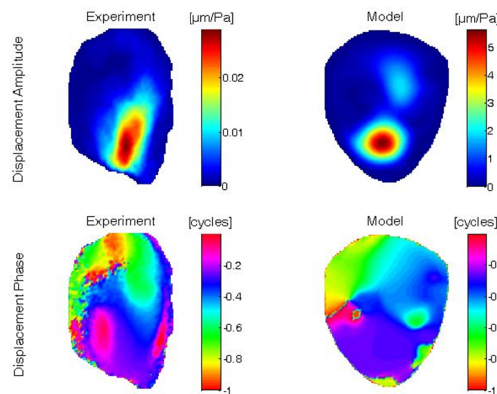


**Figure 8.** The displacement amplitude and phase of the tympanic membrane, compared for the results of the holography measurements and the optimized finite element model. The optimized model parameters were chosen to be  $[E_{TM}, E_{EC}] = [40.3, 39.6]$  MPa at 1600 Hz. Notice that the inverse analysis was obtained only by considering the normalized displacement patterns, in contrast to the absolute displacements [5].

The plots of the objective function make clear that the eardrum Young's modulus  $E_{TM}$  has a bigger influence on the objective function than the modulus of the extracolumella  $E_{EC}$ , which is not unexpected as we considered the eardrum displacements in our analysis. The optimal output values of the model lie on a curve inside a

finite region of the input domain. To find this curve a fit was carried out using a second order polynomial with two parameters  $c_1$  and  $c_2$  by minimizing the line integral along the curve. The equation describing this polynomial is

$$E_{EC} = c_1(E_{TM} - c_2)^2. \quad (3)$$

The optimal values for the two parameters are  $[c_1, c_2] = [5.92E-7, 4.85E7]$  at the chosen frequency. The minimum objective function value along the fitted line was found at  $[E_{TM}, E_{EC}] = [40.3, 39.6]$  MPa for 1600 Hz. In Fig. 8 the displacement magnitude and phase of the tympanic membrane are compared for the holography measurements and the optimized finite element model.

In addition, an inverse analysis was performed using the LDV results as input, in which the objective function is defined by Eq. (2). The input parameters are chosen to be the Young's moduli of the tympanic membrane  $E_{TM}$  and the annular ligament  $E_{AL}$ . The resulting surrogate model is shown in Fig. 9.

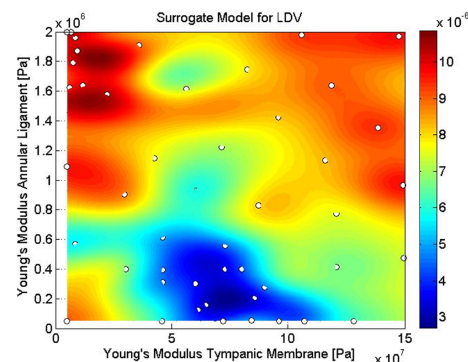


**Figure 9.** Inverse analysis on the Young's moduli of the tympanic membrane (TM) and the annular ligament (AL), using 10 of the 66 stimulus frequencies as input. The result is obtained by a surrogate modeling routine built with 48 samples. Colors on the plot represent the objective function between model and experiment as defined by Eq. (2).

In the obtained surrogate model we can identify a minimum, which is characterized by the parameter values  $[E_{TM}, E_{AL}] = [64.5, 0.156]$  MPa. Fig. 10 shows a comparison between the LDV measurements and the optimized finite element model. Notice that the cochlear load at the footplate was disabled in this calculation, since the cochlea had to be removed for the LDV measurements that served as input for this procedure.

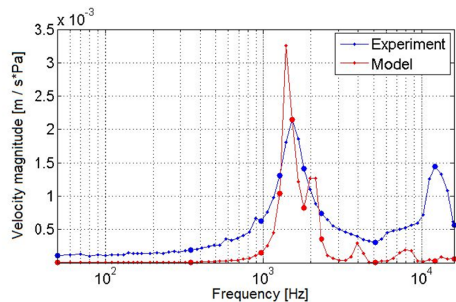


**Figure 10.** The velocity magnitude at the center of the columella footplate, compared for the results of the LDV measurements and the optimized finite element model. The optimized model parameters were chosen to be  $[E_{TM}, E_{AL}] = [64.5, 0.156]$  MPa. Notice that the inverse analysis was obtained by only considering the 10 highlighted frequencies.

#### 4. Discussion and Conclusions

In order to investigate the mechanics of complex biomechanical systems such as the avian middle ear, we believe that a multidisciplinary approach is necessary. Therefore, a combination of optical experiments and computerized finite element modeling has been used in this work. Based on contrast-enhanced high-resolution  $\mu$ CT measurements, a finite element model of the duck middle ear was constructed. Using the experimental holography and LDV data, different influential parameters were optimized by minimizing an objective function between experimental and model outcome. Using the holography results, the parameters that were chosen to be optimized are the Young's moduli of the TM and the extracolumella. The objective function was found to be minimal for parameter values of 40.3 MPa (TM) and 39.6 MPa (EC) at 1600 Hz. These were found through an inverse analysis routine, based on the MATLAB Surrogate Modeling (SUMO) Toolbox (INTEC, UGhent), as explained in detail.

The same procedure was also carried out using the LDV results as experimental input, with the isotropic Young's moduli of the tympanic membrane and the annular ligament as input parameters. The objective function was now found to be minimal for the parameter values of 64.5 MPa (TM) and 0.156 MPa (AL).

This work is the first step in the determination of the mechanical properties of the avian middle ear. Nevertheless there are several

possible improvements to be made. For instance, the acoustic stimulation of the middle ear could be modeled by acoustic-shell interaction instead of applying a uniform harmonic load at the eardrum surface. Furthermore, the relative influence and uncertainty of the different model parameters can be mapped by performing sensitivity and uncertainty analyses. Also, anisotropic, inhomogeneous, non-linear, and frequency dependent properties might be taken into account in the numerical model, that can be validated by novel static and dynamic experiments.

#### 5. References

1. R. Dooling, Avian hearing and the avoidance of wind turbines, *PhD thesis, University of Maryland, Colorado* (2002).
2. B. Moore, *Cochlear Hearing Loss: Physiological, Psychological and Technical Issues*. John Wiley & Sons Ltd., Cambridge (2007).
3. I. Arechvo et al., The ostrich middle ear for developing an ideal ossicular replacement prosthesis, *Eur. Arch. Otorhinolaryngol.*, **270** (1), 37 (2013).
4. B.C. Masschaele et al., Software tools for quantification of X-ray microtomography at the UGCT, *Nucl. Instr. & Methods in Phys. Res. A*, **580**, 442 (2007).
5. P. Muyschondt et al., Optical techniques as validation tools for finite element modeling of biomechanical structures, demonstrated in bird ear research, *AIP Proceedings*, **1600**, 330 (2014).
6. D. De Greef et al., Viscoelastic properties of the human tympanic membrane studied with stroboscopic holography and finite element modeling, *Hear. Res.*, **312**, 69 (2014).
7. K. Homma et al., Effects of ear-canal pressurization on middle-ear bone- and air-conduction responses, *Hear. Res.*, **263** (1-2), 204 (2010).
8. G. Spahn et al., Biomechanical properties of hyaline cartilage under axial load, *Zentralbl. Chir.*, **128**, 78 (2003).
9. K. Homma et al., Ossicular resonance modes of the human middle ear for bone- and air-conduction, *J. Acoust. Soc. Am.*, **125** (1), 968 (2009).
10. H. Cai et al., A biological gear in the human middle ear, *Proceedings of the COMSOL Conference*, Boston (2010).

11. M. Ravicz et al., Sound-power collection by the auditory periphery of the Mongolian gerbil *Meriones unguiculatus*: III. Effect of variations in middle-ear volume, *J. Acoust. Soc. Am.*, **101** (4), 2135 (1997).
12. S. Merchant et al., Acoustic input impedance of the stapes and cochlea in human temporal bones, *Hear. Res.*, **97**, 30 (1996).
13. D. De Greef et al., Measurement of rabbit eardrum vibration through stroboscopic digital holography, *AIP Proceedings*, **1600**, 323 (2014).
14. D. Gorissen et al., A surrogate modeling routine and adaptive sampling toolbox for computer based design, *Journal of Machine Learning Research*, **11**, 2051 (2010).

## 6. Acknowledgements

This work was financially supported by the Research Foundation Flanders (FWO) and the University of Antwerp.